THE JOURNAL OF PHYSICAL CHEMISTRY A

Article

pubs.acs.org/JPCA

Combined Crossed Molecular Beam and Ab Initio Investigation of the Reaction of Boron Monoxide (BO; $X^2\Sigma^+$) with 1,3-Butadiene ($CH_2CHCHCH_2$; X^1A_g) and Its Deuterated Counterparts

Surajit Maity, Beni B. Dangi, Dorian S. N. Parker, and Ralf. I. Kaiser*

Department of Chemistry, University of Hawai'i at Manoa, Honolulu, Hawaii 96822, United States

Hong-Mao Lin, Hai-Ping E, Bing-Jian Sun, and A. H. H. Chang*

Department of Chemistry, National Dong Hwa University, Shoufeng, Hualien 974, Taiwan

Supporting Information

ABSTRACT: The reactions of the boron monoxide (^{11}BO; $X^2\Sigma^+$) radical with 1,3-butadiene ($CH_2CHCHCH_2$; X^1A_g) and its partially deuterated counterparts, 1,3-butadiene-d_2 ($CH_2CDCDCH_2$; X^1A_g) and 1,3-butadiene-d_4 ($CD_2CHCHCD_2$; X^1A_g), were investigated under single collision conditions exploiting a crossed molecular beams machine. The experimental data were combined with the state-of-the-art ab initio electronic structure calculations and statistical RRKM calculations to investigate the underlying chemical reaction dynamics and reaction mechanisms computationally. Our investigations revealed that the reaction followed indirect scattering dynamics through the formation of $^{11}BOC_4H_6$ doublet radical intermediates via the barrierless addition of the ^{11}BO radical to the terminal carbon atom (C1/C4) and/or the central carbon atom (C2/C3) of 1,3-butadiene. The resulting long-lived $^{11}BOC_4H_6$ intermediate(s) underwent isomerization and/or unimolecular decomposition involving eventually at least two distinct atomic hydrogen loss pathways to 1,3-butadienyl-1-oxoboranes ($CH_2CHCHCH^{11}BO$) and 1,3-butadienyl-2-oxoboranes (CH_2C (^{11}BO)$CHCH_2$) in overall exoergic reactions via tight exit transition states. Utilizing partially deuterated 1,3-butadiene-d_2 and -d_4, we revealed that the hydrogen loss from the methylene moiety (CH_2) dominated with 70 ± 10% compared to an atomic hydrogen loss from the methylidyne group (CH) of only 30 ± 10%; these data agree nicely with the theoretically predicted branching ratio of 80% versus 19%.

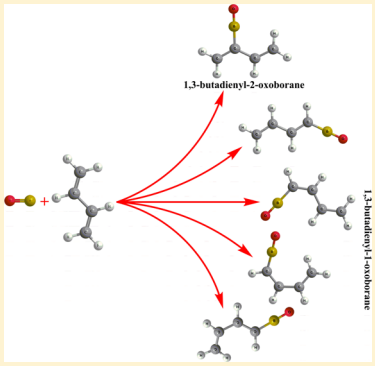

1. INTRODUCTION

During the past decade, the formation mechanisms of boron−oxygen bearing molecules has received considerable attention from the experimental and computational viewpoints in the fields of boron combustion chemistry,[1,2] reaction dynamics,[3] and physical−organic chemistry (isoelectronic reactants).[3−6] Boron combustion chemistry in particular has been studied in depth due to the potential applications of boron as a fuel additive to rocket, ramjet, and scramjet propulsion systems. Here, the oxidation of boron holds the highest energy density value of (58.7 kJ g^{-1} and 137.5 kJ cm^{-3})[1,2] and therefore is considered as a high energy propellant compared to hydrocarbon based jet propellants.[7] However, the oxidation of boron is primarily unable to reach full energy release due to the formation of an inert layer of diboron trioxide (B_2O_3) coating the nonreacted boron.[1,2] Extensive investigations, both experimentally and theoretically, have been performed to understand these boron combustion processes[2,7−15] ultimately developing chemical models to understand the gasification of the diboron trioxide (B_2O_3) layer.[15−23] Previous chemical models considered the incorporation of hydrocarbons and expanded the models to the B/C/H/O system also incorporating fluorine for an enhanced boron combustion.[15−23] Although the kinetic models developed by Zhou et al.[15] and Brown et al.[19] are the most comprehensive to date, they require experimental input parameters such as reaction products and their kinetics (rate constants). Recently, Hussmann et al. proposed a simplified boron combustion model with the help of the kinetics established by Zhou et al.[15] and the experiments done by Kuo et al.[10,24,25] concluding that more accurate experimental parameters were crucial to execute the full chemical kinetics model. Therefore, experimental and theoretical investigations of the basic bimolecular reactions relevant to boron-based combustion processes are required. Previously, our group systematically investigated the reaction dynamics of the formation of organo-boron species[26] utilizing the crossed molecular beam technique. These studies accessed the B/C/H system via the reaction of ground state boron atoms with key hydrocarbons such as acetylene (C_2H_2),[27] ethylene (C_2H_4),[28] methylacetylene (CH_3CCH),[29] allene (H_2CCCH_2),[30] dimethy-

Received: November 23, 2014
Revised: January 27, 2015
Published: January 27, 2015

DOI: 10.1021/jp511715e
J. Phys. Chem. A 2015, 119, 1094−1107

lacetylene (CH_3CCCH_3),[31] and benzene (C_6H_6).[32] However, due to the presence of oxygen in combustion processes, experimental parameters for the B/C/H/O system are also required to develop chemically complete boron combustion models. Note that the boron monoxide radical (BO) is the very first intermediate formed in the boron combustion system,[19,23,33] which can react then with the components of the hydrocarbon fuel to form B/C/H/O bearing molecules. Recently, our group has been systematically investigating the elementary reactions between boron monoxide and small unsaturated hydrocarbons such as acetylene (C_2H_2),[34] ethylene (C_2H_4),[35] methylacetylene (CH_3CCH),[36] allene (H_2CCCH_2),[37] propylene (C_3H_6),[38] dimethylacetylene (CH_3CCCH_3),[39] diacetylene (HCCCCH),[40] and benzene (C_6H_6)[41] using the crossed molecular beams technique.

Besides the combustion community, the synthesis and characterization of organyloxoboranes (RBO) has attracted considerable interest due to the presence of reactive boron−oxygen multiple bonds.[42,43] Preliminary experimental studies on organyloxoboranes depicted evidence of very strong boron−oxygen triple bond holding bond energies of typically 799 kJ mol^{-1}.[3,44−47] However, due to their intrinsic electron deficiency and polar nature, RBO undergoes cyclooligomerization at very low temperatures even at 50 K.[48] Therefore, organyloxoboranes were reported either as reactive intermediates or in cold matrixes.[44,46,49] The synthesis and characterization of organyloxoborane (RBO) as well as experimental evidence of stable oxoboranes is still sparse.[50,51] In addition, the reaction of boron monoxide radicals (BO) draws considerable interest from the physical organic community as it is isoelectronic with the cyano radical (CN).[4−6] Previously, the reaction of cyano radicals with hydrocarbons such as acetylene (C_2H_2),[52] ethylene (C_2H_4),[53] methylacetylene (CH_3CCH),[54] allene (CH_2CCH_2),[55] propylene (CH_3CHCH_2),[56] dimethylacetylene (CH_3CCCH_3),[57] 1,3-butadiene ($CH_2CHCHCH_2$),[58] and benzene (C_6H_6)[59] were explored experimentally and theoretically to unravel the chemical reaction dynamics together with the thermodynamic properties (reaction exoergicity) of the nitrile products.[3,34−41,60]

Here, we expand the studies of boron monoxide reactions and investigate the reaction dynamics of boron monoxide with 1,3-butadiene ($CH_2CHCHCH_2$; X^1A_g) together with its partially deuterated counterparts ($CH_2CDCDCH_2$; $CD_2CHCHCD_2$) to systematically elucidate the reaction dynamics of boron monoxide with unsaturated hydrocarbons under single collision reaction conditions. The present work utilizes the crossed molecular beams technique[61−66] along with ab initio electronic structure calculations and statistical RRKM calculations to investigate the reaction dynamics and the products of the title reaction. In addition, the reaction dynamics and potential energy surface of the boron monoxide 1,3-butadiene ($CH_2CHCHCH_2$) system are compared with its isoelectronic reaction of cyano radicals (CN) with 1,3-butadiene ($CH_2CHCHCH_2$) studied earlier in our laboratory.[58]

2. EXPERIMENTAL AND DATA ANALYSIS

The reaction of the ground state boron monoxide radical (BO; $X^2\Sigma^+$) with 1,3-butadiene ($CH_2CHCHCH_2$; X^1A_g) was conducted in a universal crossed molecular beams machine under single collision conditions.[61−66] Briefly, a supersonic beam of ground state boron monoxide (BO) was produced in situ via laser ablation of a boron rod at 266 nm and seeding the ablated boron in pure carbon dioxide carrier gas (CO_2, 99.99%, BOC gases).[67] The fourth harmonic output of a Spectra-Physic Quanta-Ray Pro 270 Nd:YAG laser (266 nm) operating at a repetition rate of 30 Hz with an output power of 15−20 mJ per pulse was focused on the rotating boron rod using a lens of 1500 mm focal length. The carbon dioxide gas was released by a Proch-Trickl pulsed valve with a nozzle diameter of 1 mm operating at 60 Hz with 80 μs pulse width and −350 V pulse amplitude.[68] A backing pressure of 4 atm was used, which yielded a pressure of 5×10^{-4} Torr inside the primary source chamber. The ablated boron reacted with the carbon dioxide to produce BO($X^2\Sigma^+$) possibly via atomic oxygen abstraction; the beam passed through a skimmer of diameter 1 mm. A four-slot chopper wheel operating at 120 Hz was placed 18 mm downstream from the skimmer and selected a 11.2 μs segment of the BO($X^2\Sigma^+$) beam with a peak velocity (v_p) of 1430 ± 40 ms^{-1} and speed ratio (S) of 2.3 ± 0.3. The ro-vibrational levels of the boron monoxide radical were characterized in situ via laser-induced fluorescence (LIF) spectroscopy.[69] Briefly, the $^2\Sigma^+$ electronic ground state of the boron monoxide radical was probed via the $A^2\Pi$−$X^2\Sigma^+$ transition. The (0,0) vibrational band near 425 nm was recorded by using a Nd:YAG pumped Lambda Physik Scanmate dye laser output of 10 μJ per pulse. The spectra were analyzed using the diatomic spectral simulation program developed by Tan.[70] The rotational temperature was determined to be 250 K.[69] This indicates that the ^{11}BO radicals have a maximum of 2 kJ mol^{-1} of internal energy.[35,69] The LIF spectrum of the ^{11}BO radical did not show any (1,1) vibrational band; on the basis of the noise, less than 5% of the ^{11}BO radical was suggested to reside in the ν = 1 level.[69]

The selected segment of the primary beam was crossed by a second pulsed molecular beam of 1,3-butadiene ($CH_2CHCHCH_2$, $CD_2CHCHCD_2$, and $CH_2CDCDCH_2$) perpendicularly in the interaction region. Neat 1,3-butadiene (Aldrich 99%+ and C/D/N Isotopes 98%) was released by a second Proch-Trickl pulsed valve operating at a repetition rate of 60 Hz with an 80 μs pulse width from a backing pressure of 550 Torr characterized by a peak velocity of 760 ± 20 ms^{-1} and speed ratio (S) of 8.0 ± 0.5. The collision energy between ^{11}BO($X^2\Sigma^+$) and 1,3-butadiene was determined to be 23.6 ± 1.5 kJ mol^{-1}. Note that both pulsed valves, the laser pulse, and the chopper wheel were synchronized by three digital pulse generators (Stanford Research System, DG535) with the help of two frequency dividers (Pulse Research Lab, PRL-220A). The time zero trigger originates from a photodiode, mounted on the top of the chopper wheel. The primary and the secondary pulsed valves were triggered at 1890 and 1865 μs, respectively, after the time zero trigger pulse. The laser was triggered 146 μs after the trigger pulse of the primary pulsed valve.

The reactively scattered products were monitored using a triply deferentially pumped quadrupole mass spectrometer (QMS) in the time-of-flight (TOF) mode after electron-impact ionization of the neutral species at 80 eV electron energy with an emission current of 2 mA. The extracted ions pass through a quadrupole mass filter (Extrel QC 150) operated with an oscillator frequency of 2.1 MHz. Only ions with selected mass-to-charge (m/z) passes through the quadrupole mass filter and were accelerated toward a stainless steel target coated with a thin layer of aluminum maintained at a voltage of −22.5 kV. The ions hit the surface and initiate an electron cascade until it reaches an aluminum coated organic scintillator, whose photon cascade is detected by a photomultiplier tube (PMT, Burle,

DOI: 10.1021/jp511715e
J. Phys. Chem. A 2015, 119, 1094−1107

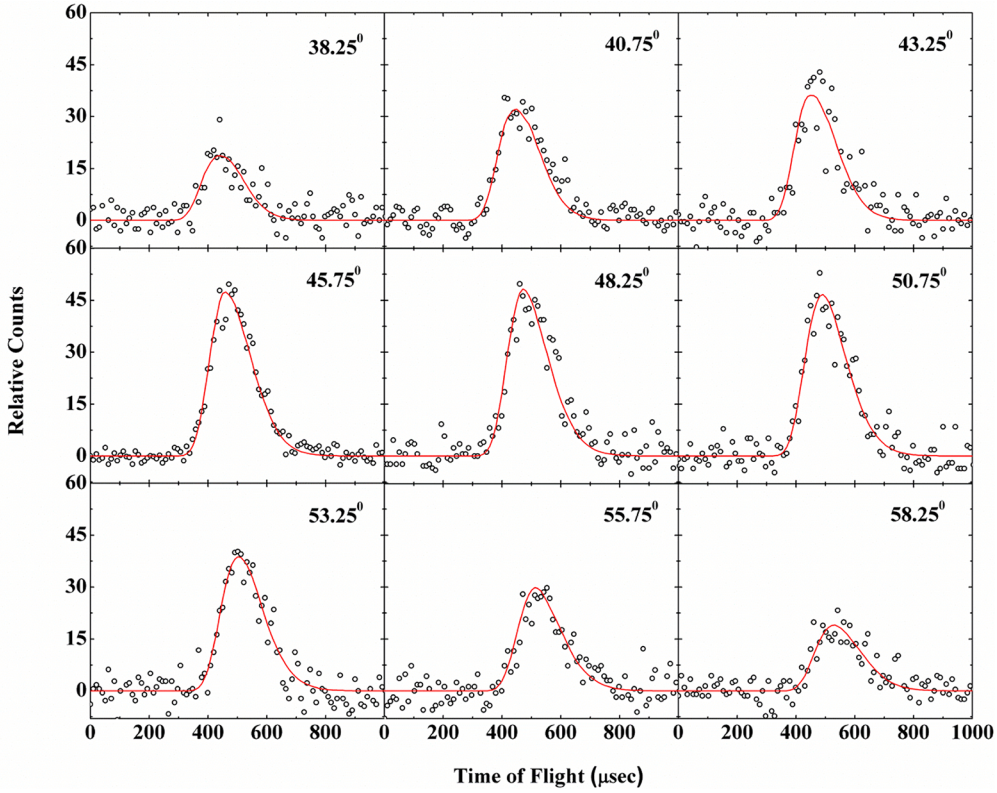

Figure 1. Time-of-flight spectra recorded at m/z = 80 ($^{11}BOC_4H_5^+$) at various angles for the reaction between boron monoxide (^{11}BO; $X^2\Sigma^+$) with 1,3-butadiene ($CH_2CHCHCH_2$; X^1A_g) at a collision energy of 23.6 ± 1.5 kJ mol^{-1}. The circles indicate the experimental data, and the solid lines indicate the calculated fit.

Model 8850) operated at −1.35 kV. The signal from the PMT was then filtered by a discriminator (Advanced Research Instruments, Model F-100TD, level: 1.6 mV) prior to feeding into a multichannel scaler (Stanford Research System SR430) to record the time-of-flight spectra.[63,65] The detector is rotatable within the plane defined by the primary and the secondary reactant beams to allow taking angular resolved TOF spectra. At each angle, up to 1.3 × 10^5 TOF spectra were collected to probe the hydrogen loss channel. The recorded TOF spectra were then integrated and normalized to extract the product angular distribution in the laboratory frame. To gain information on the reaction dynamics, the experimental data must be transformed into the center-of-mass reference frame utilizing a forward-convolution routine.[71,72] This iterative method assumes an initial choice of angular flux distribution, $T(\theta)$, and the product translational energy distribution, $P(E_T)$ in the center-of-mass frame. Laboratory TOF spectra and the laboratory angular distribution were then calculated from the $T(\theta)$ and $P(E_T)$ functions and were averaged over a grid of Newton diagrams to account for the apparatus functions and the beam spreads in velocity and direction. Best fits were obtained by iteratively refining the adjustable parameters in the center-of-mass functions within the experimental error limits of, for instance, peak velocity, speed ratio, error bars in the laboratory angular distribution. The product flux contour map, $I(\theta,u) = P(u)\,T(\theta)$, reports the intensity of the reactively scattered products (I) as a function of the CM scattering angle (θ) and product velocity (u). This plot is called the reactive *differential cross section* and gives an image of the reaction. The branching ratios of the channels were calculated using the method proposed by Krajnovich et al.[73]

3. THEORETICAL

Probable reaction paths in the reaction of boron monoxide ($BO(X^2\Sigma^+)$) with 1,3-butadiene ($CH_2CHCHCH_2$, X^1A_g) are explored by ab initio electronic structure calculations. The intermediates, transition states, and dissociation products are characterized such that their optimized geometries and harmonic frequencies are obtained at the level of the hybrid density functional theory, the unrestricted B3LYP/c-pVTZ.[74,75] The energies are refined with the coupled cluster[76−79] CCSD(T)/cc-pVTZ with B3LYP/cc-pVTZ zero-point energy corrections. The GAUSSIAN-03 program was utilized in the electronic structure calculations.[80] Further, assuming the energy is equilibrated among the molecular degrees of freedom before the reaction occurs, and provided the energy is conserved, such as in molecular beam experiments, the rate constants for the individual steps were predicted via RRKM theory. For a reaction $A^* \xrightarrow{k} A^\ddagger \rightarrow P$, where A* is the energized reactant, $A^\ddagger$ represents the transition state, and P represents the products, the rate constant $k(E)$ may be expressed as

$$k(E) = \frac{\sigma}{h}\frac{W^\ddagger(E - E^\ddagger)}{\rho(E)} \tag{1}$$

where σ is the symmetry factor, $W^\ddagger$ is the number of states of the transition state, $E^\ddagger$ is the transition state energy, and ρ is the density of states of the reactant. ρ and $W^\ddagger$ are computed by the saddle-point method; molecules are treated as collections of harmonic oscillators whose harmonic frequencies are obtained by B3LYP/cc-pVTZ as described above.[81] These rate constants were also exploited to predict the branching ratios of the reaction.[81]

DOI: 10.1021/jp511715e
J. Phys. Chem. A 2015, 119, 1094−1107

4. RESULTS

4.1. Experimental Results. The reactive scattering signal for the reaction of boron monoxide (^{11}BO; $X^2\Sigma^+$) (27 amu) with 1,3-butadiene ($CH_2CHCHCH_2$; X^1A_g) (54 amu) was recorded at the mass-to-charge ratios of m/z = 80 ($^{11}BOC_4H_5^+$) and m/z = 79 ($^{11}BOC_4H_4^+/^{10}BOC_4H_5^+$) for the atomic hydrogen and/or molecular hydrogen loss pathways. After scaling, the TOF spectra recorded at m/z = 79 depicted an identical profile with the TOF spectra recorded at m/z = 80 (Supporting Information, Figure S1). These observations alone indicate that the ions at m/z = 79 originated from the dissociative ionization of the parent at m/z = 80 ($^{11}BOC_4H_5^+$) in the electron impact ionizer of the detector. Therefore, we can conclude that in the reaction of $^{11}BO(X^2\Sigma^+)$ with 1,3-butadiene ($CH_2CHCHCH_2$; X^1A_g), the boron monoxide versus atomic hydrogen loss channel leading to the formation of $^{11}BOC_4H_5$ isomer(s) is open; further, the molecular hydrogen loss channel is closed. Selected TOF spectra for the atomic hydrogen loss channel recorded at a m/z = 80 at a collision energy of 23.6 ± 1.5 kJ mol^{-1} are depicted in Figure 1. We also attempted to monitor the products at mass-to-charge (m/z) of 66 ($^{11}BOC_3H_3^+$) to 63 ($^{11}BOC_3^+/^{10}BOC_3H^+$), which potentially arise from a methyl group loss, but did not observe any reactive scattering signal. This indicates that, in the reaction of boron monoxide (^{11}BO; 27 amu) with 1,3-butadiene ($CH_2CHCHCH_2$; 54 amu), any methyl loss channel is found to be closed or below the detection limit.

The laboratory angular distribution of the atomic hydrogen loss channel was obtained by integrating the TOF spectra taken for the $^{11}BOC_4H_5$ product(s) at m/z = 80 (Figure 2). Here, the laboratory angular distribution is extended by at least 50° in the scattering plane defined by the primary and the secondary molecular beams. The distribution peaks at 48.3 ± 1.5° close to the center-of-mass (CM) angle of 46.7 ± 2.0°. The distribution is nearly symmetric around the center-of-mass angle, which suggests that the reaction proceeds via indirect (complex forming) scattering dynamics involving $^{11}BOC_4H_6$ reaction intermediate(s).

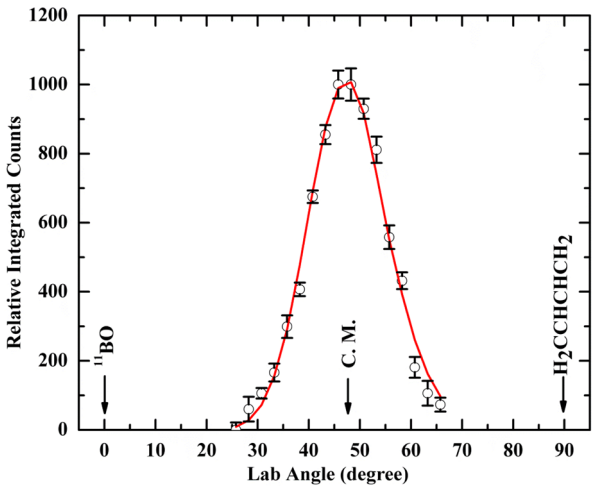

Figure 2. Laboratory angular distribution (LAB) of $^{11}BOC_4H_5$ product (m/z = 80) for the reaction of boron monoxide (^{11}BO; $X^2\Sigma^+$) with 1,3-butadiene ($CH_2CHCHCH_2$; X^1A_g) at a collision energy of 23.6 ± 1.5 kJ mol^{-1}. The circles and error bars indicate the experimental data, and the solid line indicates the calculated distribution.

Having identified the atomic hydrogen loss pathways, we are focusing our attention now on the position of the atomic hydrogen loss. Note that the chemical structure of 1,3-butadiene ($CH_2CHCHCH_2$) reactant contains two chemically different sets of hydrogen atoms, four methylene hydrogens (CH_2) positioned at two terminal carbon atoms (C1 and C4), and two methylidyne hydrogens (CH) located at the central carbon atoms (C2 and C3). Therefore, to determine the position of the atomic hydrogen loss, we utilized partially deuterated reactants, 1,3-butadiene-2,3-d_2 ($CH_2CDCDCH_2$; X^1A_g) and 1,3-butadiene-1,1,4,4-d_4 ($CD_2CHCHCD_2$; X^1A_g). First, we carried out the reaction between $CH_2CDCDCH_2$ (56 amu) and ^{11}BO (27 amu) and recorded the TOF spectra at m/z = 82 ($^{11}BOC_4D_2H_3^+$) for the atomic hydrogen loss channel from the terminal carbon atoms (C1 and C4) of 1,3-butadiene. The TOF spectra are depicted in Figure 3, clearly confirming the existence of the atomic hydrogen loss channel from the terminal carbon (C1 and C4) of 1,3-butadiene ($CH_2CHCHCH_2$). Second, we explored a potential atomic hydrogen loss from the methylidyne group (CH) of 1,3-butadiene ($CH_2CHCHCH_2$). For this, we conducted the crossed beam reaction of $CD_2CHCHCD_2$ (58 amu) with ^{11}BO (27 amu); a hydrogen loss from the methylidyne group (CH) should lead to the formation of $^{11}BOC_4D_4H$ product(s) with a mass of 84 amu. The TOF spectra taken at m/z = 84 ($^{11}BOC_4D_4H^+$) as depicted in Figure 3 confirm the presence of the atomic hydrogen loss channel from the central carbon atom (C2 and C3) of 1,3-butadiene ($CH_2CHCHCH_2$). Note that a competing deuterium loss can only be detected at mass-to-charge ratios (m/z) of 81 ($^{11}BOC_4DH_4^+$) and 83 ($^{11}BOC_4D_3H_2^+$) for 1,3-butadiene-d_2 and -d_4 systems, respectively. However, in these two systems, we have only recorded the TOF spectra for the atomic hydrogen loss channels at m/z = 82 and m/z = 84, respectively. Therefore, deuterium loss channels do not contribute to our recorded TOF spectra. Note that, for both partially deuterated 1,3-butadienes, we recorded the TOF spectra only at the center-of-mass angle because of low signal counts and the high cost of these chemicals. We analyzed the branching ratios of the two atomic hydrogen loss

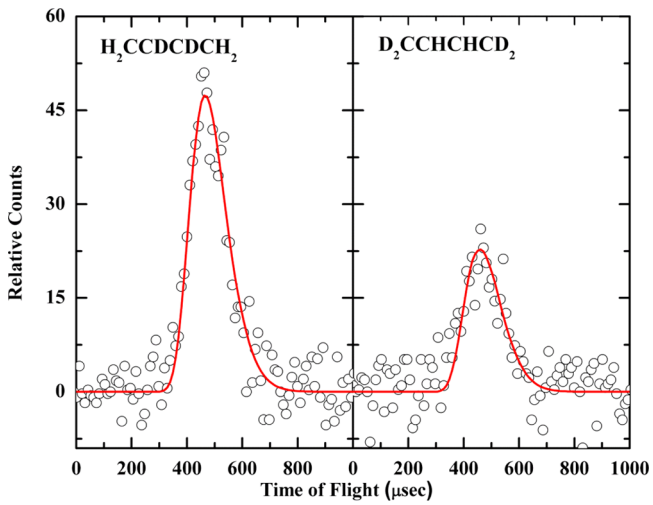

Figure 3. Time-of-flight data at the center-of-mass angles recorded for the hydrogen loss pathway in the reactions of boron monoxide (^{11}BO; $X^2\Sigma^+$) with partially deuterated 1,3-butadiene (left) $CH_2CDCDCH_2$ (X^1A_g) and (right) $CD_2CHCHCD_2$ (X^1A_g) at m/z = 82 and m/z = 84, respectively.

DOI: 10.1021/jp511715e
J. Phys. Chem. A 2015, 119, 1094−1107

channels by integrating the TOF spectra.[73] The branching ratios for the atomic hydrogen loss channels from methylene (CH_2) hydrogen (C1 and C4 carbon atoms) and methylidyne (CH) hydrogen (C2 and C3 carbon atoms), were determined to be 70 ± 10% and 30 ± 10%, respectively.

4.2. Center-of-Mass System. To elucidate the chemical dynamics of the boron monoxide−1,3-butadiene system, the laboratory data were transformed into the center-of-mass reference frame utilizing a forward convolution routine as elucidated in section 2. The laboratory data, TOF spectra and laboratory angular distribution, were fit using a single channel with a product mass combination of 80 amu ($^{11}BOC_4H_5$) and 1 amu (H). Figure 4 shows the center-of-mass angular and translational energy distributions for the title reaction. Here, the best fit center-of-mass translational energy distribution, $P(E_T)$, shows that the maximum of the flux distribution is located away from zero translational energy between 10 and 16 kJ mol^{-1}. This finding suggests the presence of a tight exit transition state (repulsive bond rupture with a significant electron rearrangement) from the decomposing complex to the product.[82] Also, as can be seen from the $P(E_T)$, the maximum translational energy (E_{max}) value is found to be 71 ± 12 kJ mol^{-1}. From the conservation of energy, we can calculate the reaction exoergicity by subtracting the collision energy (23.6 ± 1.5 kJ mol^{-1}) from E_{max}. Here, we deduce that the reaction forming $^{11}BOC_4H_5$ isomer(s) plus hydrogen (H) is exoergic by 47 ± 14 kJ mol^{-1}. Finally, the average energy released into the translational degrees of freedom is found to be 24 ± 5 kJ mol^{-1}, about 34 ± 3% of the total available energy. This order-of-magnitude is indicative of indirect (complex forming) scattering dynamics involving $^{11}BOC_4H_6$ intermediates.[82]

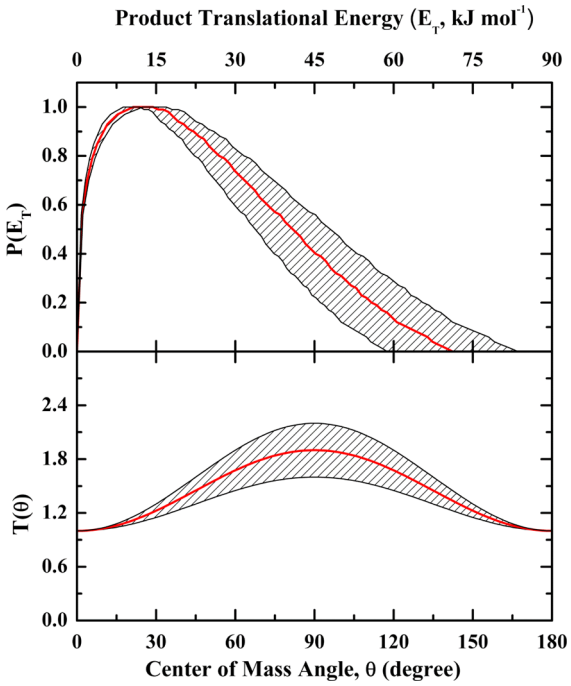

Figure 4. Center-of-mass translational energy distribution (top) and center-of-mass angular distribution (bottom) for the hydrogen loss channel of the reaction between boron monoxide (^{11}BO; $X^2\Sigma^+$) with 1,3-butadiene ($CH_2CHCHCH_2$; X^1A_g). The hatched areas indicate the acceptable lower and upper limits of the fits, and the solid red lines define best fit functions.

The center-of-mass angular distribution, $T(\theta)$, as shown in Figure 4 (bottom), provides additional information on the reaction dynamics of the title reaction. The distribution shows intensities over the whole angular range from 0° to 180° and is forward−backward symmetric with respect to 90°. The intensity over the complete scattering range is indicative of indirect scattering dynamics involving the formation of $^{11}BOC_4H_6$ collision complex(es) for the boron monoxide−1,3-butadiene system.[83] The forward−backward symmetry suggests that the lifetime of the decomposing $^{11}BOC_4H_6$ complex(es) is(are) longer than their rotation period or a symmetric exit transitions state.[83] In the case of a symmetric exit transitions state, the rotation should interconvert the emitting hydrogen atom in the decomposing complex via a proper rotation axis; hence, the probability of the leaving hydrogen atom from the decomposing complex is equal from θ and $\pi - \theta$.[83] Finally, the best fit depicts a heavily angular distribution maximum at 90°. These findings suggest geometrical constraints in the exit channel(s).[83] In this atomic hydrogen loss channel, the hydrogen atom is suggested to be emitted almost perpendicularly to the plane of the decomposing $^{11}BOC_4H_6$ complex, i.e., nearly parallel to the total angular momentum vector ("sideways scattering"). These findings are also compiled in the flux contour map (Figure 5).

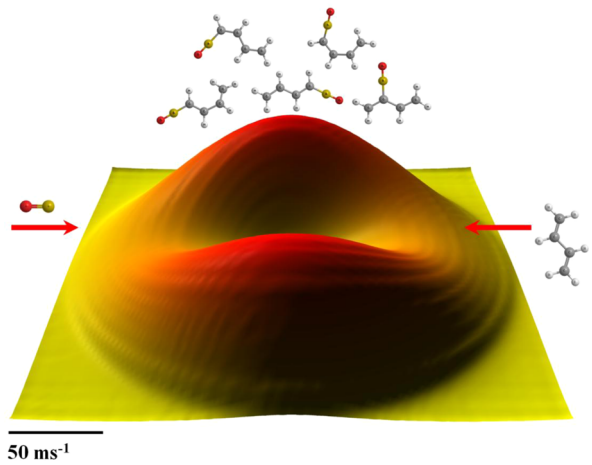

Figure 5. Flux contour maps of the atomic hydrogen loss pathway in the crossed beam reaction of boron monoxide radicals with 1,3-butadiene leading to the formation of 1,3-butadienyl-1-oxoborane ($CH_2CHCHCH^{11}BO$) and 1,3-butadienyl-2-oxoborane ($CH_2C(^{11}BO)CHCH_2$).

5. THEORETICAL RESULTS

The title reaction was also investigated computationally using ab initio electronic structure theory. The potential energy surface of the ^{11}BO plus 1,3-butadiene systems is shown in Figure 6 with the relevant structures depicted in Figures 7−9. The computation predicts that the reaction between boron monoxide and 1,3-butadiene proceeds via the barrierless addition of the boron monoxide radical with its radical center located on the boron atom to either the terminal carbon atom (C1, C4) or the central carbon atom (C2, C3) of 1,3-butadiene reactant ($CH_2CHCHCH_2$) forming $^{11}BOC_4H_6$ intermediates **i1** (−219 kJ mol^{-1}) and **i3** (−150 kJ mol^{-1}), respectively. Note that 1,3-butadiene remains in its *trans* form in the molecular beam with negligible contributions from the higher energy *cis*/

DOI: 10.1021/jp511715e
J. Phys. Chem. A 2015, 119, 1094−1107

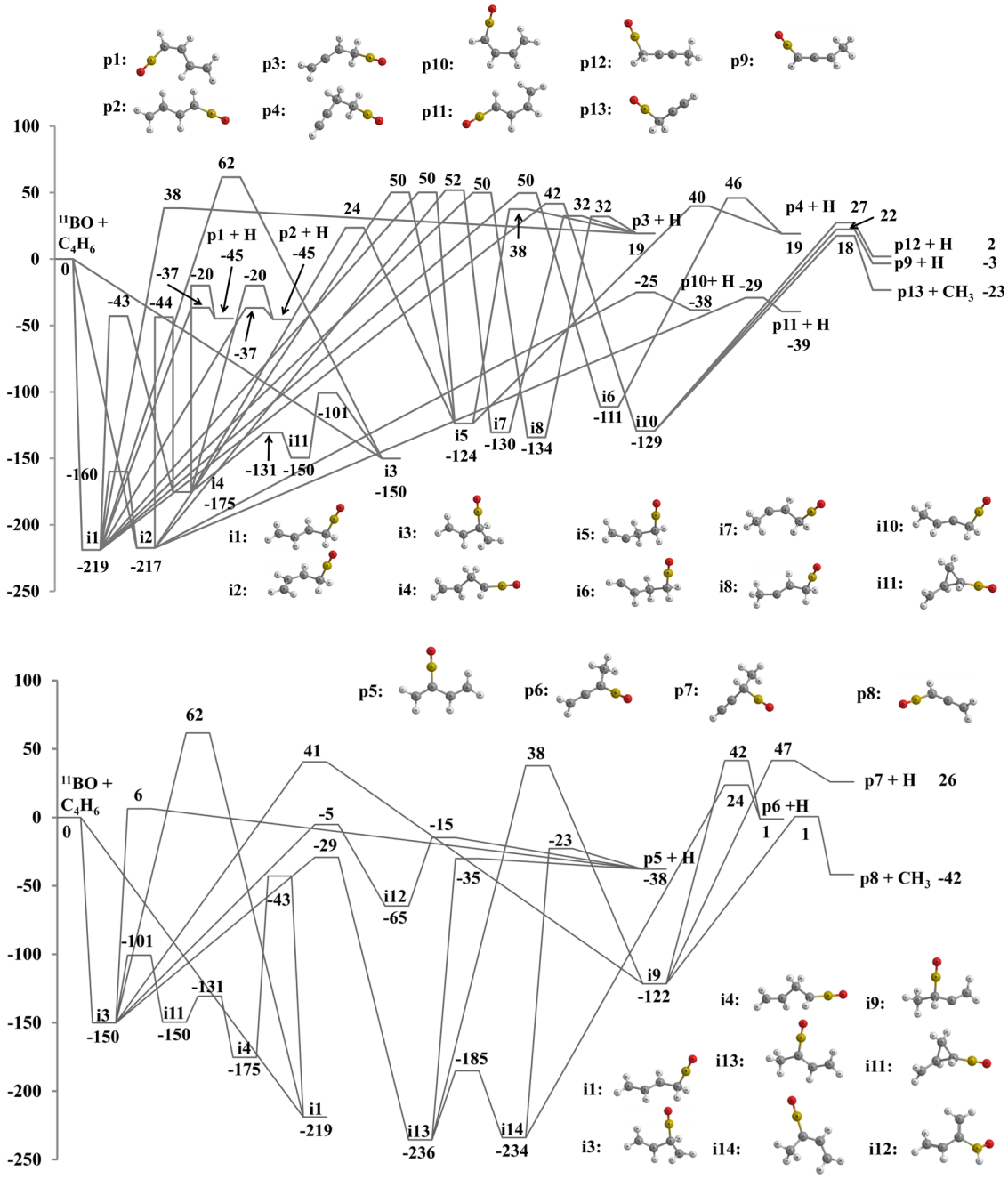

Figure 6. Schematic representation of the computed $^{11}BOC_4H_6$ potential energy surface (PES).

gauche isomers.[84] The calculation also predicts a barrierless addition of the boron monoxide radical to the terminal carbon atom of the *cis* isomer of 1,3-butadiene forming intermediate **i2** (−217 kJ mol^{-1}). In addition, intermediate **i1** can rapidly isomerize to **i2** due to the low lying transition state (−160 kJ mol^{-1}) with a barrier height of only 59/57 kJ mol^{-1} above **i1**/**i2**. Therefore, even though the population of the higher energy *cis*/*gauche* isomers is negligible, **i2** can still be accessible. Intermediates **i1** and **i2** hold the boronyl group at the terminal carbon atom of the hydrocarbon moiety. A boronyl (^{11}BO) group migration from the terminal carbon atom of **i1** to the central carbon atom to form **i3** is associated with a high energy barrier, which is located 62 kJ mol^{-1} above the separated reactants. Considering the experimental collision energy of 23.6 kJ mol^{-1}, the boron monoxide migration reaction pathway is most likely restricted. However, intermediates **i1** and **i2** can isomerize to **i3** via intermediates **i4** and **i11**. Here, **i1** and **i2** may undergo atomic hydrogen migration to form **i4** (−175 kJ mol^{-1}) via an energy barrier of 176 kJ mol^{-1}. Subsequently, **i4** undergoes cyclization to intermediate **i11** (−150 kJ mol^{-1}) via the formation of a new C1−C3 single bond; eventually **i11** isomerizes via C2−C3 bond breaking to form **i3**.

We discuss now the predicted reaction pathways related to intermediates **i1**, **i2**, and **i4**. Intermediate **i1** can undergo three competing unimolecular decomposition pathways via atomic hydrogen loss from the C1 and C3 carbon atoms of the 1,3-butadiene moiety. The atomic hydrogen elimination from the terminal C1 carbon atom can lead to the formation of substituted *trans*-1,3-butadiene products (*Z*)- and (*E*)-1,3-butadieneyl-1-oxoborane ($CH_2CHCHCH^{11}BO$; **p1** and **p2**)

DOI: 10.1021/jp511715e
J. Phys. Chem. A 2015, 119, 1094−1107

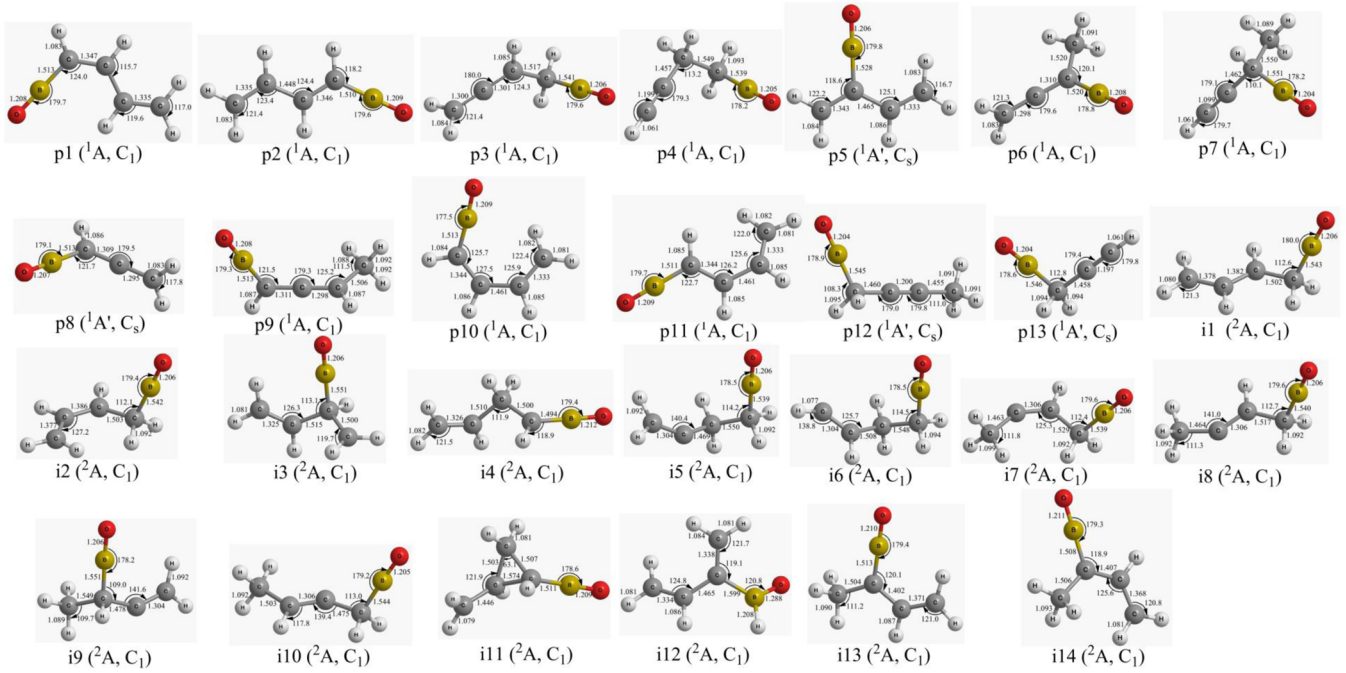

Figure 7. Structures of products and intermediates relevant to the $^{11}BOC_4H_6$ potential energy surface (PES). Angles and bond lengths are given in degrees and angstroms, respectively.

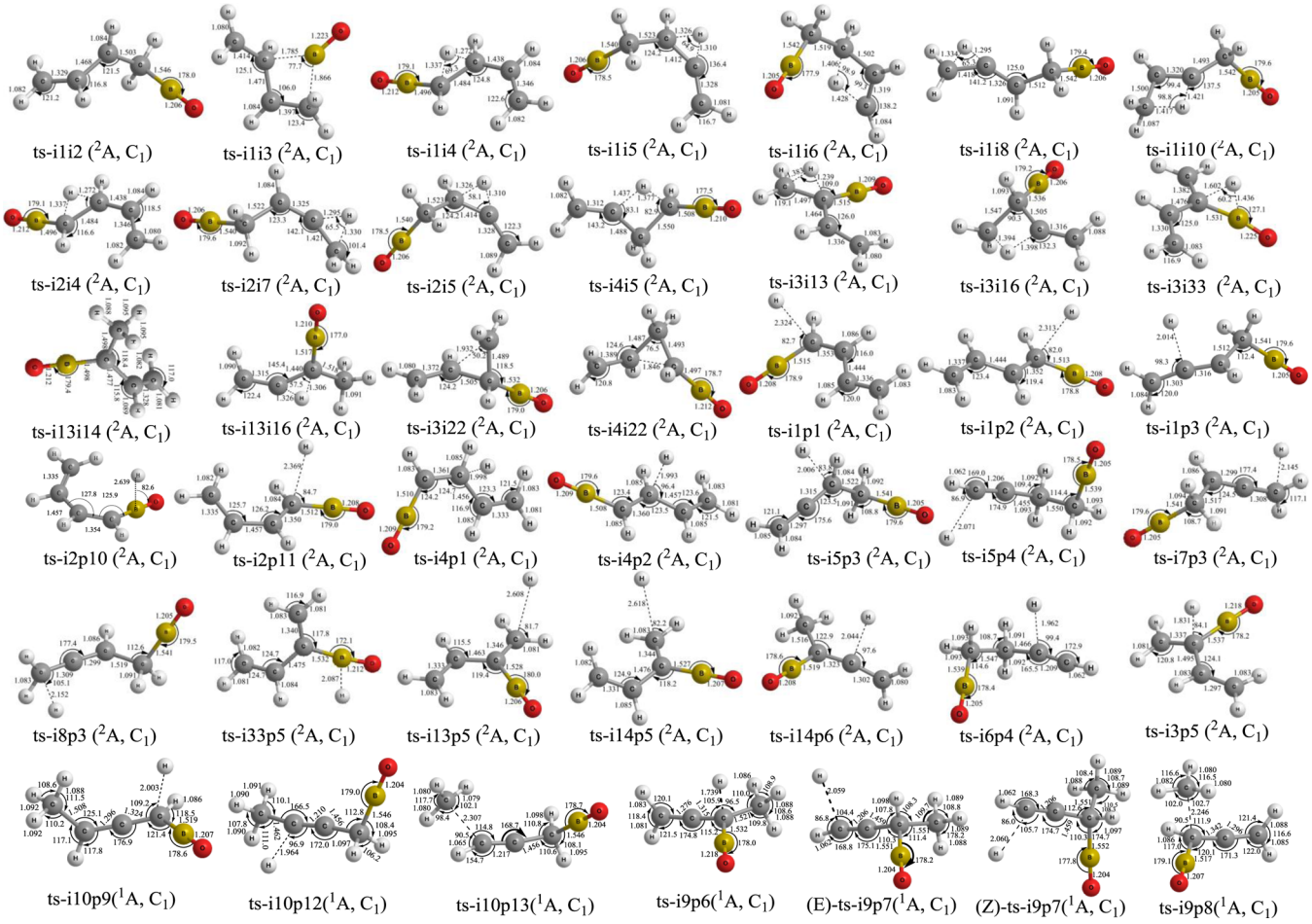

Figure 8. Structures of the transition states relevant to the $^{11}BOC_4H_6$ potential energy surface (PES). Angles and bond lengths are given in degrees and angstroms, respectively.

DOI: 10.1021/jp511715e
J. Phys. Chem. A 2015, 119, 1094−1107

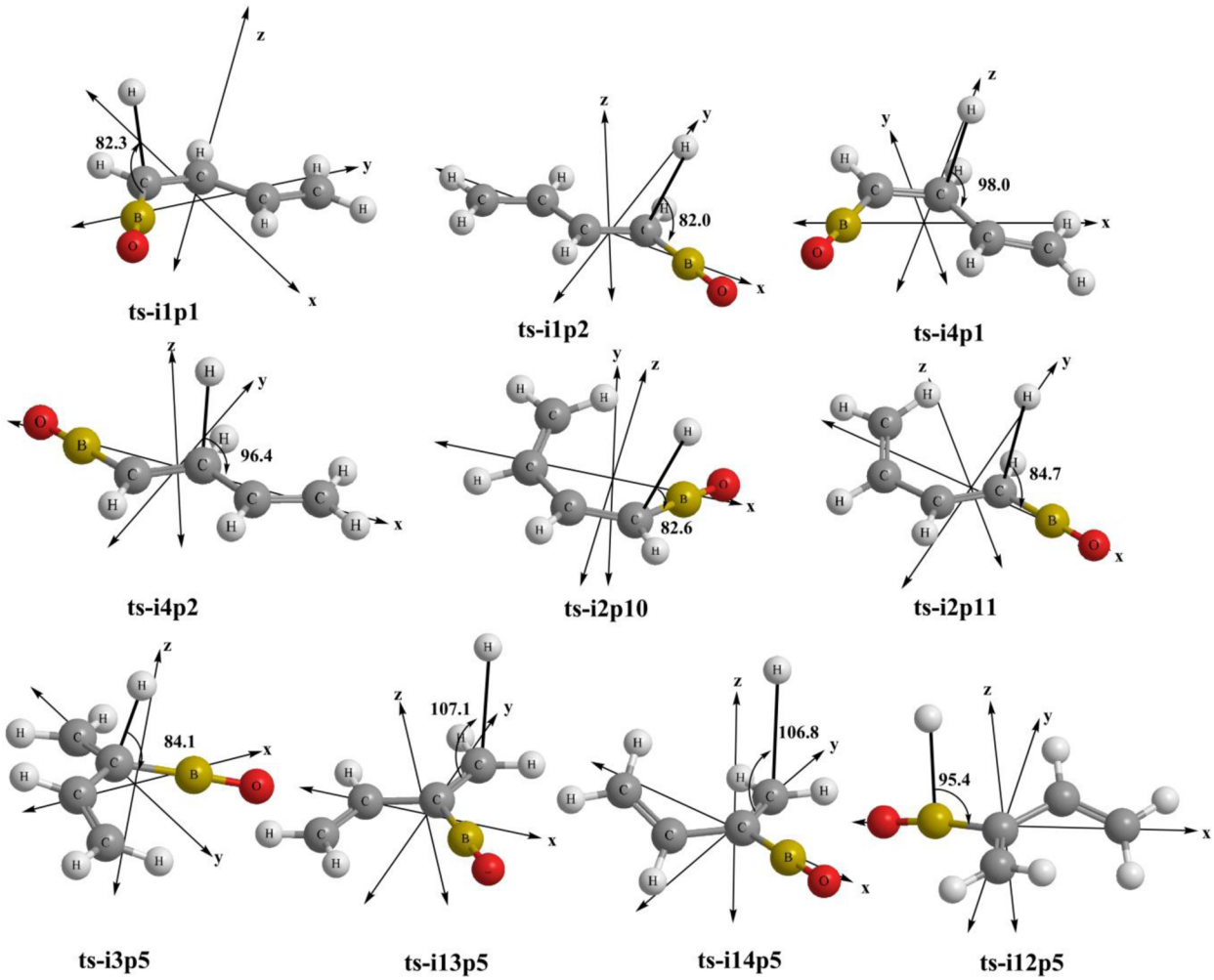

Figure 9. Geometries of the relevant exit transition states of the $^{11}BOC_4H_6$ potential energy surface (PES). Angles are given in degrees.

with overall reaction exoergicities of 45 kJ mol^{-1}. Additionally, atomic hydrogen loss from the central C3 carbon atom of **i1** can lead to the formation of substituted allene, 2,3-butadienyloxoborane ($CH_2CCHCH_2{}^{11}BO$; **p3**) in an overall endoergic reaction (19 kJ mol^{-1}). The reactions leading to **p1**, **p2**, and **p3** proceed via tight exit transition states residing 8, 8, and 19 kJ mol^{-1}, respectively, above the separated products. Intermediate **i2**, can also undergo unimolecular decompositions via atomic hydrogen elimination from the terminal carbon atom (C1) of the butadiene moiety forming substituted *cis*-1,3-butadiene products, (*Z*)- and (*E*)-1,3-butadieneyl-1-oxoborane ($CH_2CHCHCH^{11}BO$; **p10** and **p11**). These reactions proceed through tight exit transition states located 13 and 10 kJ mol^{-1} above the separated products, respectively, and are exoergic by 38 kJ mol^{-1}. An atomic hydrogen elimination from **i4** can result the formation of substituted *trans*-1,3-butadiene products, **p1** and **p2** ((*Z*)- and (*E*)-1,3-butadieneyl-1-oxoborane), as well. These reactions also proceed through tight exit transition states located 25 kJ mol^{-1} above the separated products.

Besides the above-mentioned decomposition pathways, intermediates **i1**, **i2**, and **i4** may isomerize to the intermediates **i5**−**i10** located within −124 and −134 kJ mol^{-1} below the separated reactants. Note that these isomerization reactions are associated with high energy barriers with transition states located 24−52 kJ mol^{-1} above the separated reactants. Considering the low energy barriers for the competing atomic hydrogen elimination pathways associated with **i1**, **i2**, and **i4** and the experimental collision energy of 23.6 kJ mol^{-1}, intermediates **i5**−**i10** are most likely inaccessible. Therefore, atomic hydrogen loss pathways associated with **i5**−**i10** to form **p3** (2,3-butadienyloxoborane; $CH_2CCHCH_2{}^{11}BO$), **p4** (3-butynyloxoborane; $HCCCH_2CH_2{}^{11}BO$), **p12** (2-butynyloxoborane; $CH_3CCCH_2{}^{11}BO$), **p9** (1,2-butadienyloxoborane; $CH_3CHCCH^{11}BO$), and the methyl loss pathway from **i10** to the product **p13** (2-propynyloxoborane; $HCCCH_2{}^{11}BO$) are most likely unimportant pathways in the present experimental conditions.

Now we discuss the reaction pathways associated with intermediate **i3**, which can be formed via the addition of the ^{11}BO radical to the central carbon atom (C2 and C3) of the 1,3-butadiene reactant. **i3** can undergo unimolecular decomposition via an atomic hydrogen elimination from the C2 carbon atom of the 1,3-butadiene moiety to form substituted a 1,3-butadiene product, 1,3-butadienyl-2-oxoborane ($CH_2C(^{11}BO)CHCH_2$; **p5**). The reaction proceeds via a tight exit transition state residing 44 kJ mol^{-1} above the separated products with an overall exoergicity of 39 kJ mol^{-1} with respect to the separated reactants. **i3** can also isomerize via a [1,2] hydrogen migration to the boron atom to form **i12** (−65 kJ mol^{-1}), which eventually undergoes atomic hydrogen elimination to **p5** (1,3-butadienyl-2-oxoborane). Further, **i3** can also isomerize via [1,2] hydrogen migration to the terminal carbon

DOI: 10.1021/jp511715e
J. Phys. Chem. A 2015, 119, 1094−1107

atom (C1) to form **i13** (−236 kJ mol^{-1}) by overcoming an energy barrier of 121 kJ mol^{-1}; this intermediate eventually undergoes rapid *cis*−*trans* isomerization to form **i14** (−234 kJ mol^{-1}) via a low lying transition state located only 49−51 kJ mol^{-1} above the intermediates **i14**/**i13**. Here, both **i13** and **i14** can undergo unimolecular decomposition via atomic hydrogen elimination from the terminal carbon atom (C1) to form **p5** (1,3-butadienyl-2-oxoborane) by overcoming exit transition states located 3 and 15 kJ mol^{-1} above the separated products. Intermediate **i14** may also undergo atomic hydrogen elimination from the C3 carbon atom to form substituted allene product **p6** (2,3-butadienyl-2-oxoborane; $CH_2CC(CH_3)^{11}BO$) via an overall endoergic reaction (1 kJ mol^{-1}). The reaction pathway is associated with a very high energy barrier of 258 kJ mol^{-1} and the exit transition state is positioned 24 kJ mol^{-1} above the separated reactants. Note that the statistical RRKM calculations (Supporting Information, Table S2) predicted that this reaction (**i14** → **p6**) are highly unlikely, because the rate constant of the competing decomposition pathway to **p5** is 5 orders of magnitude higher than the rate constant of **i14** → **p6** pathway; hence, they are omitted from further discussion. In addition, a [1,3] hydrogen migration (C3 to C1 carbon atom) from **i1** and/or [1,2] hydrogen migration (C3 to C2 carbon atom) from **i13** may lead to the formation of intermediate **i9** (−122 kJ mol^{-1}). These reactions are associated with transition states located about 38−41 kJ mol^{-1} above the separated reactants. Therefore, intermediate **i9** and the related decomposition pathways to the products **p6** (2,3-butadienyl-2-oxoborane), **p7** (3-propynyl-2-oxoborane; $HCCCH(CH_3)^{11}BO$), and **p8** (propadienyloxoborane) are most likely unimportant stationary points at the present experimental conditions.

Statistical RRKM calculations have also been performed to calculate the rate constants of each reaction pathway (Supporting Information, Table S2) and to eventually predict the branching ratios for the products (Supporting Information, Table S3) at a collision energy of 23.6 kJ mol^{-1}. The branching ratios of the atomic hydrogen loss products *trans*-(*Z*/*E*)-1,3-butadieneyl-1-oxoborane (**p1**, **p2**), *cis*-(*Z*/*E*)-1,3-butadieneyl-1-oxoborane (**p10**, **p11**), and 1,3-butadienyl-2-oxoborane (**p5**) are calculated to be 69%, 11%, and 19%, respectively. The branching ratios are obtained by considering an initial 100% population of either **i1** or **i3** and take into account that both initial collision complexes do isomerize via **i4** and **i11** (Supporting Information, Table S3).

6. DISCUSSION

To investigate the underlying pathways and reaction dynamics involved in the collision reactions between boron monoxide (^{11}BO; $X^2\Sigma^+$) and 1,3-butadiene ($CH_2CHCHCH_2$; X^1A_g), we are now comparing the experimental results with the theoretical data. First, let us briefly summarize the experimental results. The crossed molecular beam experiments with boron monoxide and 1,3-butadiene confirm the existence of the atomic hydrogen loss pathway leading to $^{11}BOC_4H_5$ (80 amu) and H (1 amu). Any methyl loss pathway and molecular hydrogen loss pathways were found to be closed or below the detection limit. The experiments with partially deuterated 1,3-butadiene ($CH_2CDCDCH_2$ and $CD_2CHCHCD_2$) depict two distinct atomic hydrogen loss pathways. Here, atomic hydrogen eliminations from the methylene (CH_2) group of $CH_2CDCDCH_2$ and methylidyne (CH) group of $CD_2CHCHCD_2$) lead to the formation of $^{11}BOC_4D_2H_3$ (82 amu) and $^{11}BOC_4D_4H$ (84 amu) isomers, respectively, with fractions of 70 ± 10% and 30 ± 10%, via atomic hydrogen versus boron monoxide exchange reactions. The center of mass translational energy distribution $P(E_T)$ shows a reaction exoergicity of 47 ± 14 kJ mol^{-1}. The distribution shows a peak at 8−16 kJ mol^{-1}, suggesting the presence of a tight exit transition state between the decomposing complex and the product. The center-of-mass angular distribution depicts a forward−backward symmetry, which indicates indirect scattering dynamics via long-lived $^{11}BOC_4H_6$ complexes holding lifetimes longer than their rotation period. Further, the $T(\theta)$ distribution is peaked at 90° suggesting a geometrical constraints in the exit transition state and the atomic hydrogen elimination occurs almost parallel to the total angular momentum vector.

To identify the isomers of the reaction product ($^{11}BOC_4H_5$; 80 amu), we are now comparing the predicted reaction energies with the experimental data. The electronic structure calculation predicts 11 $^{11}BOC_4H_5$ isomers. As discussed earlier, among the products, the thermodynamically accessible products are **p1**, **p2**, **p5**, **p10**, and **p11**. Note that, except for these products, alternative reaction pathways to the products are associated with transition state(s) that are located 38−52 kJ mol^{-1} above the separated reactants. Considering the experimental collision energy of 23.6 kJ mol^{-1}, these products are inaccessible and hence are skipped from further discussion. The cross molecular beam data confirm a reaction exoergicity of 47 ± 14 kJ mol^{-1}. The experimental data agree with the computed reaction exoergicities of **p1** (−45 kJ mol^{-1}), **p2** (−45 kJ mol^{-1}), **p5** (−38 mol^{-1}), **p10** (−38 kJ mol^{-1}), and **p11** (−39 kJ mol^{-1}). Note that the products, **p1**, **p2**, **p10**, and **p11**, are isomers of 1,3-butadienyl-1-oxoborane ($CH_2CHCHCH^{11}BO$) and the structures depict that one of the hydrogen atoms of the terminal carbon atoms of 1,3-butadiene ($CH_2CHCHCH_2$) is essentially replaced by the boron monoxide group. Recall that in the reaction of the boron monoxide radical with 1,3-butadiene-d_2 ($CH_2CDCDCH_2$), a predominant contribution (70 ± 10%) of the atomic hydrogen loss from the terminal carbon atoms (C1 and C4) was determined experimentally. Further, the scattering reactions between the boron monoxide radical and 1,3-butadiene-d_4, $CD_2CHCHCD_2$, indicated that 30 ± 10% of the hydrogen atom is lost from the central carbon atoms (C2 and C3) as well. Here, a similar comparison of the structures of the reactants with the products reveal that isomer **p5** holds the ^{11}BO group at the C2 carbon atom of the 1,3-butadiene moiety. On the basis of the above observations, we can conclude that, in the reaction between boron monoxide and 1,3-butadiene, at least one of the products **p1**, **p2**, **p10**, and **p11** is formed via the atomic hydrogen elimination from the terminal carbon atom (CH_2 group) and **p5** is formed via the via the atomic hydrogen elimination from the central carbon atom (CH group) of the 1,3-butadiene reactant. The formation of these isomers is exoergic by between 38 and 45 kJ mol^{-1}, hence nicely correlating with the experimental findings of 47 ± 14 kJ mol^{-1}. Further, the exit transition states to form these isomers are all tight (8−44 kJ mol^{-1}); the existence of tight exit transition states nicely correlates with the experimental predictions based on the off-zero peaking of the center-of-mass translational energy distribution.

Having identified the ^{11}BO versus hydrogen atom exchange reaction products, we are now proposing the underlying reaction pathways by combining the experimental findings with the electronic structure and statistical calculations. The

DOI: 10.1021/jp511715e
J. Phys. Chem. A 2015, 119, 1094−1107

molecular structures of products, **p1**, **p2**, **p10**, and **p11** (1,3-butadienyl-1-oxoborane) propose an addition of the boron monoxide radical to the terminal carbon atoms of the 1,3-butadiene reactant; the structure of the product **p5** depicts that the boronyl group is attached to the central carbon atoms of the 1,3-butadiene reactant. These findings propose that the reaction between boron monoxide radical and 1,3-butadiene follows indirect scattering dynamics and is initiated by an addition of the boron monoxide radical with its radical center located on the boron atom to the C1/C4 and the C2/C3 carbon atom of the 1,3-butadiene reactant, resulting in the formation of $^{11}BOC_4H_6$ intermediates **i1** and **i3**, respectively. Intermediate **i1** can rapidly isomerize to **i2** via a low energy barrier. Both **i1** and **i2** decompose via atomic hydrogen loss from the terminal carbon atom attached to the boronyl group forming isomers of 1,3-butadieneyl-1-oxoborane ($CH_2CHCHCH^{11}BO$), **p1**/**p2** and **p10**/**p11**, respectively. Note that on the basis of our experiments alone we cannot predict to what extent intermediates **i1** and **i3** isomerize to each other prior to atomic hydrogen loss.

Further, the optimized geometries of the exit transition states (**ts-i1p1**, **ts-i1p2**, **ts-i2p10**, and **ts-i2p11**) connecting intermediates **i1** and **i2** with products **p1**/**p2** and **p10**/**p11** suggest a direction of the atomic hydrogen emission almost perpendicularly to the molecular plane of the decomposing complex (Figure 9). Recall that this geometry was predicted on the basis of the shape (distribution maximum at 90°) of the center-of-mass angular distribution of the atomic hydrogen loss pathway (Figure 4). In addition, intermediate **i4**, formed either via atomic hydrogen migration from **i1** and **i2** and/or via addition of ^{11}BO radical to the central carbon atoms (**i3**) followed by isomerization via the cyclic intermediate **i11**, may also loose atomic hydrogen to form **p1** and **p2** (1,3-butadieneyl-1-oxoborane). These product channels are also associated with tight exit transition states, located 25 kJ mol^{-1} above the separated products. The above observations indicate a possible minor contribution from the reaction pathways **i4** → **p1** and **i4** → **p2** toward the formation of **p1** and **p2**. The above statement also gets support from the $^{11}BOC_4H_6$ PES. Here, **ts-i1p1** and **ts-i1p2** are stabilized by 17 kJ mol^{-1} compared to **ts-i4p1** and **ts-i4p2** and the thermodynamically favorable positions clearly demonstrate **i1** → **p1**/**p2** to be the dominant reaction pathways to the formation of **p1** and **p2**.

Now we discuss the formation pathways of the product 1,3-butadieneyl-2-oxoborane (**p5**), which shows an addition of ^{11}BO group attached to the central (C2/C3) carbon of the 1,3-butadiene reactant. The above information suggests that **p5** can only be formed from intermediates related to **i3** where ^{11}BO is attached to the central carbon atom. Intermediate **i3** can undergo (i) unimolecular decomposition via atomic hydrogen loss, (ii) isomerization to form **i12** followed by decomposition via atomic hydrogen loss, and (iii) isomerization to **i13** and **i14** followed by decomposition via an atomic hydrogen loss to form **p5**. Here, the reaction pathway **i3** → **p5** is associated with a tight exit transition state located at 44 kJ mol^{-1} above the separated products. The reaction pathway **i3** → **i12** → **p5** is connected with an energy barrier of 145 kJ mol^{-1} (**ts-i3i12**). In the reaction pathways **i13**/**i14** → **p5**, an atomic hydrogen migration from C2 to C1 carbon atoms of **i3** resulted in the formation of **i13**, which can rapidly interchange with **i14** via *cis*−*trans* isomerization by overcoming a low lying energy barrier of 51/49 kJ mol^{-1}. **i13**/**i14** can undergo atomic hydrogen elimination from the terminal methyl group to yield **p5** with associated exit transition states located 3 and 15 kJ mol^{-1} above the separated products, respectively. Note that the energy barriers associated with **i3** → **p5** and **i3** → **i12** → **p5** pathways are in the range 145−156 kJ mol^{-1} and are 50 kJ mol^{-1} lower in energy than the energy barriers associated with **i13**/**i14** → **p5** pathways (201−211 kJ mol^{-1}). The above statement proposes that **i3** → **p5** and **i3** → **i12** → **p5** pathways are most likely the dominating atomic hydrogen loss pathways to the formation of 1,3-butadieneyl-2-oxoborane (**p5**) due to the associated lower energy barriers. Our statistical RRKM calculations also agreed with the above statement, and about 60−96% of **p5** are formed via these reaction pathways (Supporting Information, Table S3).

Finally, we comment on the experimental finding of the closed methyl loss channels. The theoretical calculations predict the formation of two methyl loss products, **p8** and **p13** via overall exoergic reactions with energies of −42 and −23 kJ mol^{-1}, respectively. At our collision energy, these reactions are energetically feasible. The formation of **p8** and **p13**, is linked to the population of the intermediates **i9** and **i10**, respectively. Recall that **i9** can be formed via either [1,3] and/or [1,2] atomic hydrogen migration from **i3** and **i13** via transition states located 41 and 38 kJ mol^{-1} above the separated reactants, respectively. Similarly, **i10** can be achieved only via [1,3] hydrogen atom migration from **i1** by overcoming a transition state located 42 kJ mol^{-1} above the separated reactants. These transition states are energetically inaccessible at a collision energy of 23.6 kJ mol^{-1}, indicating that intermediates **i9** and **i10**, are unimportant intermediates at the present experimental conditions. Therefore, the experimental finding of closed methyl loss channels is justified.

Therefore, we can conclude that unimolecular decomposition via atomic hydrogen loss in the reaction of boron monoxide and 1,3-butadiene results in the formation of boronyl substituted 1,3-butadiene products, 1,3-butadieneyl-1-oxoborane (**p1**, **p2**, **p10**, and **p11**) and 1,3-butadieneyl-2-oxoborane (**p5**). Here, the dominant reaction pathways to form the isomers of 1,3-butadienyl-1-oxoborane (**p1**, **p2**, **p10**, and **p11**) are found to be the unimolecular decomposition pathways via atomic hydrogen loss of the methylene hydrogens (CH_2) positioned at two terminal carbon atoms (C1 and C4) of the 1,3-butadiene reactants. Among them, **p1**/**p2** are most likely the dominant hydrogen loss products due to the energetically favorable positions of the exit transition states [**ts-i1p1** (−37 kJ mol^{-1}), **ts-i1p2** (−37 kJ mol^{-1}) versus **ts-i2p10** (−25 kJ mol^{-1}) and **ts-i2p11** (−29 kJ mol^{-1})]. The statistical RRKM calculations also support the above statement and the dominant yield of **p1**/**p2** with fractions of 69% of the total atomic hydrogen loss products; the contribution of **p10**/**p11** is about 11% the total atomic hydrogen loss products. The statistical calculations also predict that the atomic hydrogen loss channel to form 1,3-butadieneyl-2-oxoborane (**p5**) is found to be only 19%. Product **p5** can be formed via atomic hydrogen loss of the methylidyne hydrogens (CH) positioned at the two central carbon atoms (C2 and C3) of the 1,3-butadiene reactants. The lower percentage of **p5** can be explained as (i) a lower number of methylidyne hydrogens compared to methylene hydrogens (2 versus 4) and (ii) the energetically less favorable position of the exit transition state [e.g., **ts-i3p5** (6 kJ mol^{-1}) versus **ts-i1p1** (−37 kJ mol^{-1})]. Recall that, from the reactions between boron monoxide radical and partially deuterated 1,3-butadiene ($CD_2CHCHCD_2$ and $CH_2CDCDCH_2$), a predominant contribution (70 ± 10%) of atomic hydrogen loss from the two

DOI: 10.1021/jp511715e
J. Phys. Chem. A 2015, 119, 1094−1107

terminal carbon atoms (methylene hydrogens) and a minor contribution (30 ± 10%) of atomic hydrogen from the central carbon atoms (methylidyne hydrogens) were experimentally determined. Our statistical RRKM calculations agree with the experimental findings with major contribution (80%) of atomic hydrogen loss from the terminal carbon atoms (1,3-butadieneyl-1-oxoborane; **p1**, **p2**, **p10**, and **p11**) and minor (19%) contribution from the central carbon atoms (1,3-butadieneyl-2-oxoborane; **p5**).

As we have mentioned earlier, the ^{11}BO ($X^2\Sigma^+$) and CN ($X^2\Sigma^+$) radicals are isoelectronic and a comparison of their reactions with 1,3-butadiene will be interesting from the physical organic chemistry viewpoint. The reaction of 1,3-butadiene with cyano radical (CN; $X^2\Sigma^+$) have previously been investigated experimentally and theoretically by our group.[58] The reaction between 1,3-butadiene with CN($X^2\Sigma^+$) radicals underwent indirect scattering dynamics via barrierless addition of the cyano radical to the terminal carbon atom of the 1,3-butadiene reactant via its radical center located at the carbon atom to form $CH_2CHCHCH_2CN$. Similarly, the reaction of $^{11}BO(X^2\Sigma^+)$ radicals with 1,3-butadiene involve indirect scattering dynamics and a barrierless addition of the ^{11}BO radical with its radical center located at the boron atom to the terminal atom of the 1,3-butadiene reactant leads to the formation of intermediate $CH_2CHCHCH_2{}^{11}BO$. These doublet radical intermediates, $CH_2CHCHCH_2X$ (X = CN, ^{11}BO), are stabilized by 267 (X = CN) and 219 kJ mol^{-1} (X = ^{11}BO), and these energetics imply the formation of a stronger carbon−carbon (X = CN) bond compared to a weaker carbon−boron (X = ^{11}BO) single bond; bond strengths differ by typically 50 kJ mol^{-1}. For both systems, the atomic hydrogen elimination from the terminal carbon atoms lead to the formation of substituted 1,3-butadiene product with molecular formula $CH_2CHCHCHX$ (X = CN, ^{11}BO). In the case of the CN($X^2\Sigma^+$) plus 1,3-butadiene reaction, the product $CH_2CHCHCHCN$ is found to be the predominant product (∼99.9%). However, the similar product, $CH_2CHCHCH^{11}BO$, formed in the ^{11}BO ($X^2\Sigma^+$) + 1,3-butadiene reaction is found to be only 70 ± 10% of the total atomic hydrogen loss products. As discussed above, an addition of the ^{11}BO radical to the central carbon atoms (C2/C3) of the 1,3-butadiene reactant is followed by atomic hydrogen elimination and can lead to the formation of $CH_2C(^{11}BO)CHCH_2$ with a fraction of 30 ± 10% of the total atomic hydrogen loss products. The formation reaction of $CH_2CHCHCHCN$ is found to be exoergic by 96 kJ mol^{-1} whereas boronyl substituted 1,3-butadiene ($CH_2CHCHCH^{11}BO$ and $CH_2C(^{11}BO)CHCH_2$) are found to be exoergic by only 38−45 kJ mol^{-1}. The enhanced exoergicity of the cyano radical reaction product is likely due to the effect of an enhanced carbon−carbon bond strength and higher yield of the cyano versus atomic hydrogen exchange channel from the C1/C4 carbon atoms compared to the weaker carbon−boron single bond strength.

7. SUMMARY

The crossed molecular beam reaction of boron monoxide (^{11}BO; $X^2\Sigma^+$) with 1,3-butadiene ($CH_2CHCHCH_2$; X^1A_g) was investigated at a collision energy of 23.6 ± 1.5 kJ mol^{-1} under single collision conditions and was correlated with ab initio electronic structure calculations and RRKM calculations. The scattering dynamics were found to be indirect and proceeded via barrierless addition of boron monoxide radical with its radical center located at the boron atom to either the terminal carbon atoms (C1/C4) and/or the central carbon atoms (C2/C3) of 1,3-butadiene ($CH_2CHCHCH_2$) reactant, forming $^{11}BOC_4H_6$ intermediates. The resulting $^{11}BOC_4H_6$ doublet radical intermediates underwent isomerization and/or unimolecular decomposition involving two distinct atomic hydrogen loss pathways forming four isomers of 1,3-butadienyl-1-oxoborane ($CH_2CHCHCH^{11}BO$; **p1**, **p2**, **p10**, and **p11**) together with 1,3-butadienyl-2-oxoborane ($CH_2C(^{11}BO)CHCH_2$; **p5**). Utilizing the 1,3-butadiene-2,3-d_2 reactant ($CH_2CDCDCH_2$), we revealed that the addition of $^{11}BO(X^2\Sigma^+)$ to the C1/C4 carbon atom of 1,3-butadiene was followed by an atomic hydrogen loss from the methylene (CH_2) group attached to the boronyl group (^{11}BO) leading to the formation of major reaction products 1,3-butadienyl-1-oxoborane ($CH_2CHCHCH^{11}BO$). The experiments with 1,3-butadiene-1,1,4,4-d_4 reactant ($CD_2CHCHCD_2$) exposed that an addition of $^{11}BO(X^2\Sigma^+)$ to the C2/C3 carbon atom of 1,3-butadiene was terminated via an atomic hydrogen elimination from the methylidyne (CH) group attached to the boronyl group (^{11}BO), leading to the product 1,3-butadienyl-2-oxoborane ($CH_2C(^{11}BO)CHCH_2$). The branching ratios for the loss of methylene (CH_2) hydrogen atom and the loss of methylidyne (CH) hydrogen atom of 1,3-butadiene were derived experimentally to be 70 ± 10% and 30 ± 10% and theoretically 80% and 19%, respectively. A comparison of the title reaction with the isoelectronic CN ($X^2\Sigma^+$) plus 1,3-butadiene reaction revealed several similarities, such as the formation pathways and chemical bonding of the predominant products $CH_2CHCHCHCN$ and 1,3-butadienyl-1-oxoborane ($CH_2CHCHCH^{11}BO$). The striking difference between these isoelectronic systems are the formation of 1,3-butadienyl-2-oxoborane ($CH_2C(^{11}BO)CHCH_2$) in the present experiments; however, a similar product was unidentified in the CN ($X^2\Sigma^+$) plus 1,3-butadiene reaction.

■ ASSOCIATED CONTENT

Supporting Information

Time-of-flight spectra, Cartesian coordinates (Å) of reactants, intermediates, products, and transition states optimized at CCSD(T)-fc/cc-pVTZ, and relative energies in kJ mol^{-1} with respect to reactants are available. Also the rate constant of each reaction pathway at the collision energy 23.6 kJ mol^{-1} and branching ratios of the products are listed. This material is available free of charge via the Internet at http://pubs.acs.org

■ AUTHOR INFORMATION

Notes

The authors declare no competing financial interest.

■ ACKNOWLEDGMENTS

This work was supported by the Air Force Office of Scientific Research, grant FA9550-12-1-0213. Computer resources at the National Center for High-Performance Computer of Taiwan were utilized in the calculations.

■ REFERENCES

(1) Young, G.; Sullivan, K.; Zacharia, M. R.; Yu, K. Combustion Characteristic of Boron Nanoparticles. *Combust. Flame* **2009**, *156*, 322−333.

(2) Ulas, A.; Kuo, K. K.; Gotzmer, C. Ignition and Combustion of Boron Particles in Fluorine Containing Environment. *Combust. Flame* **2001**, *127*, 1935−1957.

DOI: 10.1021/jp511715e
J. Phys. Chem. A 2015, 119, 1094−1107

(3) Parker, D. S. N.; Mebel, A. M.; Kaiser, R. I. The Role of Isovalency in the Reactions of the Cyano (CN), Boron Monoxide (BO), Silicon Nitride (SiN), and Ethynyl (C_2H) Radicals with Unsaturated Hydrocarbons Acetylene (C_2H_2) and Ethylene (C_2H_4). *Chem. Soc. Rev.* **2014**, *43*, 2701−2713.
(4) Li, S.-D.; Guo, J.-C.; Ren, G.-M. Density Functional Theory Investigations on Boronyl-Substituted Ethylenes $C_2H_{4-m}(BO)_m$ (m = 1−4) and Acetylenes $C_2H_{2-m}(BO)_m$ (m = 1, 2). *J. Mol. Struct.* **2007**, *821*, 153−159.
(5) Ollivier, C.; Renaud, P. Organoboranes as a Source of Radicals. *Chem. Rev.* **2001**, *101*, 3415−3434.
(6) Papakondylis, A.; Mavridis, A. Structure and Bonding of the Polytopic Molecule Li[BO]. A Theoretical Investigation. *J. Phys. Chem. A* **2001**, *105*, 7106−7110.
(7) Hinchen, J. J. Kinetics for the Quenching and Relaxation of Boron Oxide. *J. Chem. Phys.* **1993**, *99*, 4403−4410.
(8) Antaki, P.; Williams, F. A. Observations on the Combustion of Boron Slurry Droplets in Air. *Combust. Flame* **1987**, *67*, 1−8.
(9) King, M. K. Ignition and Combustion of Boron Particles and Clouds. *J. Spacecr. Rockets* **1982**, *19*, 294−306.
(10) Yeh, C. L.; Kuo, K. K. Ignition and Combustion of Boron Particles. *Prog. Energy Combust. Sci.* **1996**, *22*, 511−541.
(11) Turns, S. R.; Holl, J. T.; Solomon, A. S. P.; Faeth, G. M. Gasification of Boron Oxide Drops in Combustion Gases. *Combust. Sci. Technol.* **1985**, *43*, 287−300.
(12) Li, S. C.; Williams, F. A. Combustion of Boron-Based Solid Propellants and Solid Fuels. In *Combustion of Boron-Based Solid Propellants and Solid Fuels*; Kuo, K. K., Pein, R., Eds.; CRC Press,: Boca Raton, FL, 1993; p 248.
(13) Macek, A.; Semple, J. M. Combustion of Boron Particle at Elevated Pressures. *Proc. Combust. Inst.* **1971**, *13*, 859−868.
(14) Macek, A. Combustion of Boron Particles: Experiments and Theory. *Proc. Combust. Inst.* **1972**, *14*, 1401−1411.
(15) Zhou, W.; Yetter, R. A.; Dryer, F. L.; Rabitz, H.; Brown, R. C.; Kolb, C. E. Multi-phase Model for Ignition and Combustion of Boron Particles. *Combust. Flame* **1999**, *117*, 227−243.
(16) Yetter, R.; Rabitz, H.; Dryer, F.; Brown, R.; Kolb, C. Kinetics of High-Temperature B/O/H/C Chemistry. *Combust. Flame* **1991**, *83*, 43−62.
(17) Yetter, R.; Dryer, F.; Rabitz, H. A Comprehensive Reaction Mechanism For Carbon Monoxide/Hydrogen/Oxygen Kinetics. *Combust. Sci. Technol.* **1991**, *79*, 97−128.
(18) Brown, R. C.; Kolb, C. E.; Cho, S. Y.; Yetter, R. A.; Dryer, F. L.; Rabitz, H. Kinetic Model for Hydrocarbon-assisted Particulate Boron Combustion. *Int. J. Chem. Kinet.* **1994**, *26*, 319−332.
(19) Brown, R. C.; Kolb, C. E.; Yetter, R. A.; Dryer, F. L.; Rabitz, H. Kinetic Modeling and Sensitivity Analysis for B/H/O/C/F Combination Systems. *Combust. Flame* **1995**, *101*, 221−238.
(20) Yetter, R. A.; Dryer, F. L.; Rabitz, H.; Brown, R. C.; Kolb, C. E. Effect of Fluorine on the Gasification Rate of Liquid Boron Oxide Droplets. *Combust. Flame* **1998**, *112*, 387−403.
(21) Zhou, W.; Yetter, R. A.; Dryer, F. L.; Rabitz, H.; Brown, R. C.; Kolb, C. E. Ignition and Combustion of Boron Particles in Fluorine Containing System. *Chem. Phys. Proc. Combust.* **1996**, 495−498.
(22) Zhou, W.; Yetter, R. A.; Dryer, F. L.; Rabitz, H.; Brown, R. C.; Kolb, C. E. Effect of Fluorine on the Combustion of "Clean" Surface Boron Particles. *Combust. Flame* **1998**, *112*, 507−521.
(23) Brown, R. C.; Kolb, C. E.; Rabitz, H.; Cho, S. Y.; Yetter, R. A.; Dryer, F. L. Kinetic Model of Liquid B_2O_3 Gasification in a Hydrocarbon Combustion Environment: I. Heterogeneous Surface Reaction. *Int. J. Chem. Kinet.* **1991**, *23*, 957−970.
(24) Hussmann, B.; Pfitzner, M. Extended Combustion Model for Single Boron Particles - Part II: Validation. *Combust. Flame* **2010**, *157*, 822−833.
(25) Hussmann, B.; Pfitzner, M. Extended Combustion Model for Single Boron Particles - Part I: Theory. *Combust. Flame* **2010**, *157*, 803−821.
(26) Balucani, N.; Zhang, F.; Kaiser, R. I. Elementary Reactions of Boron Atoms with Hydrocarbons - Toward the Formation of Organo-Boron Compounds. *Chem. Rev.* **2010**, *110*, 5107−5127.
(27) Zhang, F.; Gu, X.; Kaiser, R. I.; Bettinger, H. A Reinvestigation of the Gas Phase Reaction of Boron Atoms, $^{11}B(^2P_j)/^{10}B(^2P_j)$ with Acetylene, C_2H_2 ($X_1\Sigma_g^+$). *Chem. Phys. Lett.* **2007**, *450*, 178−185.
(28) Zhang, F.; Gu, X.; Kaiser, R. I.; Balucani, N.; Huang, C. H.; Kao, C. H.; Chang, A. H. H. A Crossed Beam and Ab Initio Study of the Reaction of Atomic Boron with Ethylene. *J. Phys. Chem. A* **2008**, *112*, 3837−3845.
(29) Zhang, F.; Kao, C. H.; Chang, A. H. H.; Gu, X.; Guo, Y.; Kaiser, R. I. A Crossed Molecular Beam Study on the Reaction of Boron Atoms with Methylacetylene and Partially Deuterated Methylacetylene. *ChemPhysChem* **2008**, *9*, 95−105.
(30) Zhang, F.; Sun, H. L.; Chang, A. H. H.; Gu, X.; Kaiser, R. I. Crossed Molecular Beam Study on the Reaction of Boron Atoms, $B(^2P_j)$, with Allene, $H_2CCCH_2(X^1A_1)$. *J. Phys. Chem. A* **2007**, *111*, 13305−13310.
(31) Sillars, D.; Kaiser, R. I.; Galland, N.; Hannachi, Y. Crossed-Beam Reaction of Boron Atoms, B (^2P_j), with Dimethylacetylene, CH_3CCCH_3 (X^1A_{1g}): Untangling the Reaction Dynamics to Form the 1,2-Dimethylene-3-bora-cyclopropane Molecule. *J. Phys. Chem. A* **2003**, *107*, 5149−5156.
(32) Zhang, F.; Guo, Y.; Gu, X.; Kaiser, R. I. A Crossed Molecular Beam Study on the Reaction of Boron Atoms, $B(^2P_j)$, with Benzene, $C_6H_6(X^1A_{1g})$, and D6-Benzene $C_6D_6(X^1A_{1g})$. *Chem. Phys. Lett.* **2007**, *440*, 56−63.
(33) Bauer, S. H. Oxidation of B, BH, BH_2, and B_mH_n Species: Thermochemistry and Kinetics. *Chem. Rev.* **1996**, *96*, 1907−1916.
(34) Parker, D. S. N.; Zhang, F.; Maksyutenko, P.; Kaiser, R. I.; Chang, A. H. H. A Crossed Beam and Ab Initio Investigation of the Reaction of Boron Monoxide (BO) with Acetylene (C_2H_2). *Phys. Chem. Chem. Phys.* **2011**, *13*, 8560−8570.
(35) Parker, D. S. N.; Zhang, F.; Maksyutenko, P.; Kaiser, R. I.; Chen, S. H.; Chang, A. H. H. A Crossed Beam and Ab Initio Investigation On The Formation of Vinyl Boron Monoxide (C_2H_3BO) via Reaction of Boron Monoxide (BO) with ethylene (C_2H_4). *Phys. Chem. Chem. Phys.* **2012**, *14*, 11099−11106.
(36) Maity, S.; Parker, D. S. N.; Dangi, B. B.; Kaiser, R. I.; Fau, S.; Perera, A.; Bartlett, R. J. A Crossed Molecular Beam and Ab-Initio Investigation of the Reaction of Boron Monoxide (BO; $X^2\Sigma^+$) with Methylacetylene (CH_3CCH; X^1A_1) − Competing Atomic Hydrogen and Methyl Loss Pathways. *J. Phys. Chem. A* **2013**, *117*, 11794−11807.
(37) Maity, S.; Parker, D. S. N.; Kaiser, R. I.; Ganoe, B.; Fau, S.; Perera, A.; Bartlett, R. J. Gas-Phase Synthesis of Boronylallene ($H_2CCCH(BO)$) under Single Collision Conditions: A Crossed Molecular Beams and Computational Study. *J. Phys. Chem. A* **2014**, *118*, 3810−3819.
(38) Maity, S.; Dangi, B. B.; Parker, D. S. N.; Kaiser, R. I.; An, Y.; Sun, B.-J.; Chang, A. H. H. A Combined Crossed Molecular Beam and Ab Initio Investigation of the Multi-Channel Reaction of Boron Monoxide (BO; $X^2\Sigma^+$) with Propylene (CH_3CHCH_2; X^1A'): Competing Atomic Hydrogen and Methyl Loss Pathways. *J. Phys. Chem. A* **2014**, *118*, 9632−9645.
(39) Kaiser, R. I.; Maity, S.; Dangi, B. B.; Su, Y.-S.; Sun, B. J.; Chang, A. H. H. A Crossed Molecular Beam and Ab Initio Investigation of the Exclusive Methyl Loss Pathway in the Gas Phase Reaction of Boron Monoxide (BO; $X^2\Sigma^+$) with Dimethylacetylene (CH_3CCCH_3; X^1A_{1g}). *Phys. Chem. Chem. Phys.* **2014**, *16*, 989−997.
(40) Parker, D. S. N.; Balucani, N.; Stranges, D.; Kaiser, R. I.; Mebel, A. M. A Crossed Beam and ab Initio Investigation on the Formation of Boronyldiacetylene ($HCCCC^{11}BO$; $X^1\Sigma^+$) via the Reaction of the Boron Monoxide Radical (^{11}BO; $X^2\Sigma^+$) with Diacetylene (C_4H_2; $X_1\Sigma_g^+$). *J. Phys. Chem. A* **2013**, *117*, 8189−8198.
(41) Parker, D. S. N.; Dangi, B. B.; Balucani, N.; Stranges, D.; Mebel, A. M.; Kaiser, R. I. Gas-Phase Synthesis of Phenyl Oxoborane (C_6H_5BO) via the Reaction of Boron Monoxide with Benzene. *J. Org. Chem.* **2013**, *78*, 11896−11900.

DOI: 10.1021/jp511715e
J. Phys. Chem. A 2015, 119, 1094−1107

(42) Fischer, R. C.; Power, P. P. π-Bonding and the Lone Pair Effect in Multiple Bonds Involving Heavier Main Group Elements: Developments in the New Millennium. *Chem. Rev.* **2010**, *110*, 3877−3923.
(43) Wang, Y.; Hu, H.; Zhang, J.; Cui, C. Comparison of Anionic and Lewis Acid Stabilized N-Heterocyclic Oxoboranes: Their Facile Synthesis from a Borinic Acid. *Angew. Chem., Int. Ed.* **2011**, *50*, 2816−2819.
(44) Bock, H.; Cederbaum, L.; Niessen, W. v.; Paezzold, P.; Rosmus, P.; Solouki, B. Methylboron Oxide, $H_3C—B≡O$. *Angew. Chem., Int. Ed.* **1989**, *28*, 88−90.
(45) Kawashima, Y.; Endo, E.; Kawaguchi, K.; Hirota, E. Detection and Equilibrium Molecular Structure of a Short-lived Molecule, HBO, by Microwave Spectroscopy. *Chem. Phys. Lett.* **1987**, *135*, 441−445.
(46) Lanzisera, D. V.; Andrews, L. Reactions of Laser-Ablated Boron Atoms with Methanol. Infrared Spectra and ab Initio Calculations of CH_3BO, CH_2BOH, and CH_2BO in Solid Argon. *J. Phys. Chem. A* **1997**, *101*, 1482−1487.
(47) Andrews, L.; Burkholder, T. R. Infrared Spectra of Boron Atom-Water Molecule Reaction Products Trapped in Solid Argon. *J. Phys. Chem.* **1991**, *95*, 8554−8560.
(48) Bettinger, H. F. Reversible Formation of Organyl(oxo)boranes (RBO) (R = C_6H_5 or CH_3) from Boroxins ($(RBO)_3$): A Matrix Isolation Study. *Organometallics* **2007**, *26*, 6263−6267.
(49) Ito, M.; Tokitoh, N.; Okazaki, R. A Novel Approach to an Oxoborane and Its Lewis Base Complex. *Tetrahedron Lett.* **1997**, *38*, 4451−4454.
(50) Chang, Y.; Li, Q.-S.; Xie, Y.; King, R. B.; Schaefer, H. F., III. Binuclear Iron Boronyl Carbonyls Isoelectronic with the Well-Known Decacarbonyldimanganese. *New J. Chem.* **2012**, *36*, 1022−1030.
(51) Chang, Y.; Li, Q.-S.; Xie, Y.; King, R. B. Prospects for Three-Electron Donor Boronyl (BO) Ligands and Dioxodiborene (B_2O_2) Ligands as Bridging Groups in Binuclear Iron Carbonyl Derivatives. *Inorg. Chem.* **2012**, *51*, 8904−8915.
(52) Huang, L. C. L.; Asvany, O.; Chang, A. H. H.; Balucani, N.; Lin, S. H.; Lee, Y. T.; Kaiser, R. I.; Osamura, Y. Crossed Beam Reaction of Cyano Radicals with Hydrocarbon Molecules. IV. Chemical Dynamics of Cyanoacetylene (HCCCN; $X^1\Sigma^+$) Formation from Reaction of $CN(X^2\Sigma^+)$ with Acetylene, $C_2H_2(X^1\Sigma^+_g)$. *J. Chem. Phys.* **2000**, *113*, 8656−8666.
(53) Balucani, N.; Asvany, O.; Chang, A. H. H.; Lin, S. H.; Lee, Y. T.; Kaiser, R. I.; Osamura, Y. Crossed Beam Reaction of Cyano Radicals with Hydrocarbon Molecules. III. Chemical Dynamics of Vinyl Cyanide (C_2H_3CN; $X\ ^1A'$) Formation From Reaction of $CN(X\ ^2\Sigma^+)$ with Ethylene, $C_2H_4(X\ ^1A_g)$. *J. Chem. Phys.* **2000**, *113*, 8643−8655.
(54) Huang, L. C. L.; Balucani, N.; Lee, Y. T.; Kaiser, R. I.; Osamura, Y. Crossed Beam Reaction of the Cyano Radical, $CN(X^2\Sigma^+)$, with Methylacetylene, CH_3CCH (X^1A_1): Observation of Cyanopropyne, CH_3CCCN (X^1A_1), and Cyanoallene, $H_2CCCHCN$ (X^1A'). *J. Chem. Phys.* **1999**, *111*, 2857−2860.
(55) Balucani, N.; Asvany, O.; Kaiser, R. I.; Osamura, Y. Formation of Three C_4H_3N Isomers from the Reaction of $CN(X^2\Sigma^+)$ with Allene, H_2CCCH_2 (X^1A_1), and Methylacetylene, CH_3CCH (X^1A_1): A Combined Crossed Beam and Ab Initio Study. *J. Phys. Chem. A* **2002**, *106*, 4301−4311.
(56) Gu, X.; Zhang, F.; Kaiser, R. I. Reaction Dynamics on the Formation of 1- and 3-Cyanopropylene in the Crossed Beams Reaction of Ground State Cyano Radicals (CN) with Propylene (C_3H_6) and Its Deuterated Isotopologues. *J. Phys. Chem. A* **2008**, *112*, 9607−9613.
(57) Balucani, N.; Asvany, O.; Chang, A. H. H.; Lin, S. H.; Lee, Y. T.; Kaiser, R. I.; Bettinger, H. F.; Schleyer, P. V. R.; Schaefer, H. F., III. Crossed beam Reaction of Cyano Radicals with Hydrocarbon Molecules. II. Chemical Dynamics of 1-Cyano-1-Methylallene ($CNCH_3CCCH_2$; X^1A') Formation from Reaction of $CN(X^2\Sigma^+)$ with Dimethylacetylene, CH_3CCCH_3 (X^1A_1'). *J. Chem. Phys.* **1999**, *111*, 7472−7479.
(58) Morales, S. B.; Bennett, C. J.; Le Picard, S. D.; Canosa, A.; Sims, I. R.; Sun, B. J.; Chen, P. H.; Chang, A. H. H.; Kislov, V. V.; Mebel, A. M. A Crossed Molecular Beam, Low-Temperature Kinetics, and Theoretical Investigation of the Reaction of the Cyano Radical (CN) with 1, 3-Butadiene (C_4H_6). A Route to Complex Nitrogen-bearing Molecules in Low-Temperature Extraterrestrial Environments. *Astrophys. J.* **2011**, *742*, 26−35.
(59) Balucani, N. A. O.; Chang, A. H. H.; Lin, S. H.; Lee, Y. T.; Kaiser, R. I.; Bettinger, H. F.; Schleyer, P. V. R.; Schaefer, H. F., III. Crossed Beam Reaction of Cyano Radicals with Hydrocarbon Molecules. I. Chemical Dynamics of Cyanobenzene (C_6H_5CN; X^1A_1) and Perdeutero Cyanobenzene (C_6D_5CN; X^1A_1) Formation from Reaction of $CN(X^2\Sigma^+)$ with Benzene, $C_6H_6(X^1A_{1g})$, and D6-Benzene, $C_6D_6(X^1A_{1g})$. *J. Chem. Phys.* **1999**, *113*, 7457−7471.
(60) Kaiser, R. I.; Mebel, A. M. On the Formation of Polyacetylenes and Cyanopolyacetylenes in Titan's Atmosphere and Their Role in Astrobiology. *Chem. Soc. Rev.* **2012**, *41*, 5490−5501.
(61) Gu, X.; Guo, Y.; Zhang, F.; Mebel, A. M.; Kaiser, R. I. Reaction Dynamics of Carbon-Bearing Radicals in Circumstellar Envelopes of Carbon Stars. *Faraday Discuss.* **2006**, *133*, 245−275.
(62) Gu, X.; Guo, Y.; Kaiser, R. I. Mass Spectrum of the Butadiynyl Radical (C_4H; $X^2\ \Sigma^+$). *Int. J. Mass Spectrom.* **2005**, *246*, 29−34.
(63) Gu, X. B.; Guo, Y.; Kawamura, E.; Kaiser, R. I. Design of a Convection-Cooled, Cluster-Based Voltage Divider Chain for Photomultiplier Tubes. *Rev. Sci. Instrum.* **2005**, *76*, 083115.
(64) Guo, Y.; Gu, X.; Kaiser, R. I. Mass Spectrum of the 1-Butene-3-yne-2-yl Radical (i-C_4H_3; X_2A'). *Int. J. Mass Spectrom.* **2006**, *249/250*, 420−425.
(65) Guo, Y.; Gu, X.; Kawamura, E.; Kaiser, R. I. Design of a Modular and Versatile Interlock System for Ultrahigh Vacuum Machines: A Crossed Molecular Beam Setup as a Case Study. *Rev. Sci. Instrum.* **2006**, *77*, 034701.
(66) Kaiser, R. I. Experimental Investigation on the Formation of Carbon-Bearing Molecules in the Interstellar Medium via Neutral-Neutral Reactions. *Chem. Rev.* **2002**, *102*, 1309−1358.
(67) Gu, X.; Guo, Y.; Kawamura, E.; Kaiser, R. I. Characteristics and Diagnostics of an Ultrahigh Vacuum Compatible Laser Ablation Source for Crossed Molecular Beam Experiments. *J. Vac. Sci. Technol.* **2006**, *24*, 505−511.
(68) Proch, D.; Trickl, T. A High-Intensity Multi-Purpose Piezoelectric Pulsed Molecular Beam Source. *Rev. Sci. Instrum.* **1989**, *60*, 713−716.
(69) Maksyutenko, P.; Parker, D. S. N.; Zhang, F.; Kaiser, R. I. An LIF Characterization of Supersonic BO and CN Radical Sources for Crossed Beam Studies. *Rev. Sci. Instrum.* **2011**, *82*, 083107.
(70) Tan, X. *CyberWit*, 1.4.1.1 ed., 2004.
(71) Vernon, M. *LBL Report-12422*; Lawrence Berkeley Laboratory: Berkeley, CA, 1981.
(72) Weis, P. S. *Ph.D. Thesis*, University of California, Berkley, 1986.
(73) Krajnovich, D.; Huisken, F.; Zhang, Z.; Shen, Y. R.; Lee, Y. T. Competition Between Atomic and Molecular Chlorine Elimination in the Infrared Multiphoton Dissociation of CF_2Cl_2. *J. Chem. Phys.* **1982**, *77*, 5977−5989.
(74) Becke, A. D. Density-functional thermochemistry. III. The Role of Exact Exchange. *J. Chem. Phys.* **1993**, *98*, 5648−5652.
(75) Lee, C.; Yang, W.; Parr, R. G. Development of the Colle-Salvetti Correlation-Energy Formula into a Functional of the Electron Density. *Phys. Rev. B: Condens. Matter* **1988**, *37*, 785−789.
(76) Deegan, M. J. O.; Knowles, P. J. Perturbative Corrections to Account for Triple Excitations in Closed and Open Shell Coupled Cluster Theories. *Chem. Phys. Lett.* **1994**, *227*, 321−326.
(77) Hampel, C.; Peterson, K. A.; Werner, H. J. A Comparison of the Efficiency and Accuracy of the Quadratic Configuration Interaction (QCISD), Coupled Cluster (CCSD), and Brueckner Coupled Cluster (BCCD) Methods. *Chem. Phys. Lett.* **1992**, *190*, 1−12.
(78) Knowles, P. J.; Hampel, C.; Werner, H. J. Coupled Cluster Theory for High Spin, Open Shell Reference Wave Functions. *J. Chem. Phys.* **1993**, *99*, 5219−5227.

DOI: 10.1021/jp511715e
J. Phys. Chem. A 2015, 119, 1094−1107

(79) Purvis, G. D., III; Bartlett, R. J. A Full Coupled-Cluster Singles and Doubles Model: the Inclusion of Disconnected triples. *J. Chem. Phys.* **1982**, *76*, 1910−1918.
(80) Frisch, M. J.; Trucks, G. W.; Schlegel, H. B.; Scuseria, G. E.; Robb, M. A.; Cheeseman, J. R.; Zakrzewski, V. G.; Montgomery, J. A.; Stratmann, R. E.; Burant, J. C.; et al. *Gaussian 03*, Revision C.02; Gaussian, Inc.: Wallingford, CT, 2004.
(81) Chang, A. H. H.; Mebel, A. M.; Yang, X. M.; Lin, S. H.; Lee, Y. T. Ab Initio/RRKM Approach toward the Understanding of Ethylene Photodissociation. *J. Chem. Phys.* **1998**, *109*, 2748−2761.
(82) Kaiser, R. I.; Mebel, A. M. The Reactivity of Ground-State Carbon Atoms with Unsaturated Hydrocarbons in Combustion Flames and in the Interstellar Medium. *Int. Rev. Phys. Chem.* **2002**, *21*, 307−356.
(83) Miller, W. B.; Safron, S. A.; Herschbach, D. R. Exchange Reactions of Alkali Atoms with Alkali Halides. Collision Complex Mechanism. *Disc. Faraday Soc.* **1967**, *44*, 108−122.
(84) Szalay, P. G.; Lischka, H.; Karpfen, A. Relative Stabilities of the s-Cis and Gauche Structures of 1,3-Butadiene. *J. Phys. Chem.* **1989**, *93*, 6629−6631.

DOI: 10.1021/jp511715e
J. Phys. Chem. A 2015, 119, 1094−1107